The temperature-induced transition from 3d to 1d hopping conduction in porous amorphous $Si_{1-c}Mn_c$

1997 J. Phys.: Condens. Matter 9 889

(http://iopscience.iop.org/0953-8984/9/4/009)

J. Phys.: Condens. Matter **9** (1997) 889–899. Printed in the UK PII: S0953-8984(97)75342-6

The temperature-induced transition from 3d to 1d hopping conduction in porous amorphous $Si_{1-c}Mn_c$

A I Yakimov†‡, A V Dvurechenskii†, N P Stepina†, L A Scherbakova†, C J Adkins‡, V Z Chorniy‡, V A Dravin§ and R Groetzschel‖

† Institute of Semiconductor Physics, Siberian Branch of the Russian Academy of Sciences, Prospekt Lavrent'eva 13, 630090 Novosibirsk, Russia

‡ Cavendish Laboratory, University of Cambridge, Madingley Road, Cambridge CB3 0HE, UK

§ P N Lebedev Physical Institute, Russian Academy of Sciences, 117924, Moscow, Russia

‖ Research Centre Rossendorf Incorporated, Institute for Ion Beam Physics and Material Research, POB 510119, D-01314 Dresden, Germany

Received 12 June 1996, in final form 21 October 1996

Abstract. We have investigated variable-range hopping conduction in amorphous $Si_{1-c}Mn_c$ ($c = 4$ and 7 at.%) samples obtained by ion implantation and treatment by anodic etching in HF solution—porous silicon. As temperature is reduced, we find a crossover from the $\exp[-(T_0/T)^{1/4}]$ Mott form to a simply activated law, $\exp(-\Delta E/kT)$. This behaviour is attributed to a temperature-induced transition from 3d to 1d hopping conduction in a network of weakly interconnected silicon quantum 'wires'. The mean diameter of the silicon wires, $D = 5$–6 nm, was deduced from analysis of the conductivity data and is in agreement with XTEM and STM observations. It was found that the density of states in the porous material is smaller than in the compact material due to broadening of the impurity band caused by lateral confinement in the silicon wires.

1. Introduction

Unaided, HF acid etches silicon extremely slowly, at a rate of only nanometres per hour. Driving an electric current between the acid electrolyte and the silicon sample speeds up the process, but leaves an array of deep, narrow pores that run perpendicular to the silicon surface. The pore structure has been explained in terms of available paths for the etching current. Each pore is surrounded by an insulating layer of material depleted of electrons.

Since the discovery of visible room-temperature photoluminescence in porous silicon (PS) [1, 2], this material has often been classed as a low-dimensional semiconductor. The unusual optical properties of PS are discussed in terms of quantum-size effects in a network of one-dimensional (1d) silicon pillars which are confined by surrounding pores and which have weak interconnections between them (figure 1(*a*)). It has been established [1, 2] that the conducting silicon remaining after electrochemical etching is usually in the form of thin wires, with cross-sectional dimensions of nanometre scale, and which are small enough to produce quantum-size effects in the Si band structure.

There have been several attempts to create 1d conducting samples by simply restricting the lateral dimensions of an inversion layer or of modulation-doped devices (see [3] and references therein). This has been accomplished by using very narrow gates, etching mesa structures, or by pinching an accumulation layer between two diffused junctions. The

0953-8984/97/040889+11$19.50

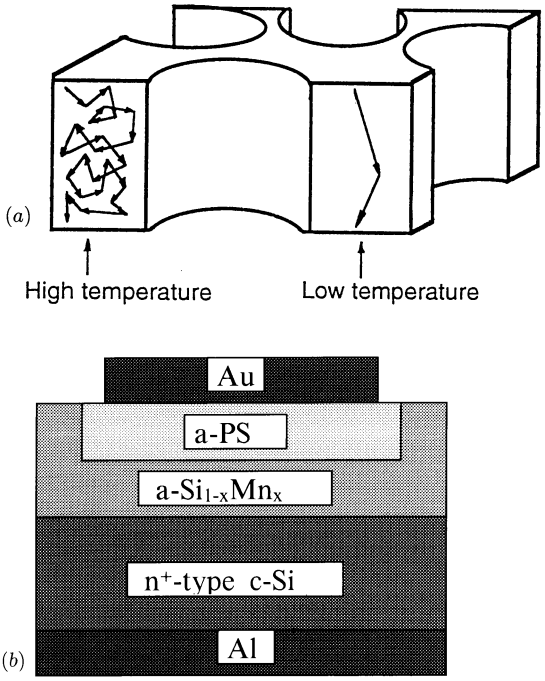

Figure 1. (*a*) A schematic representation of the structure of porous silicon. Arrows show the motion of electrons at high temperatures (small hopping length, 3d hopping) and low temperatures (large hopping length, 1d hopping). (*b*) The cross-section of the test structure.

electrolysis of silicon is a new and simple method for fabricating low-dimensional systems. Recent studies of the temperature, bias voltage and magnetic field dependence of variable-range hopping (VRH) conduction in undoped amorphous PS in the temperature range $T = 300$–140 K have revealed some properties of 1d disordered systems [4]. A problem has been the fractal structure of PS which disguises the 1d nature of charge transport at high temperatures. In this paper we will describe the temperature dependence of conductance in porous amorphous $Si_{1-c}Mn_c$ ($c = 4$ and 7 at.%) alloys. The high impurity concentration allowed us to extend the measurements to lower temperatures ($\approx$20 K) and observe directly for the first time the transition from 3d to 1d regimes of VRH transport.

2. Experimental details

Figure 1(*b*) shows a schematic diagram of the porous structure. The amorphous layers of $Si_{1-c}Mn_c$ with thickness $L_0 \approx 0.3$ μm were formed on degenerate (3 mΩ cm) n-type silicon (111) wafers by implanting Mn^+ ions. A homogeneous distribution of the impurity across the layer thickness was ensured by varying the ion energy in the range 20–300 keV. An Al coating was evaporated on the back of the wafers to improve ohmic contact. The anodization was carried out in a solution of (42% HF):H_2O:C_3H_7OH (1:2:2 by volume) at a constant current density of $j = 10$ or 15 mA cm^{-2} for $t = 6$–24 s. The PS layers grown in this way were about $L = 0.06$–0.24 μm thick with porosity $P = 50$–60%. The porosity and thickness were measured gravimetrically by weighing the samples before and after the electrochemical dissolution and after removal of the porous layer in KOH. A top contact of

Au was evaporated on the PS at a pressure of 10^{-2} Pa at a glancing geometry at an angle of $\varphi = 30^\circ$ between the molecular beam and the plane of the wafer. Increase of φ above 45° results in a sudden decrease of the sample resistance showing that the Au then reaches the Si moving through the pores.

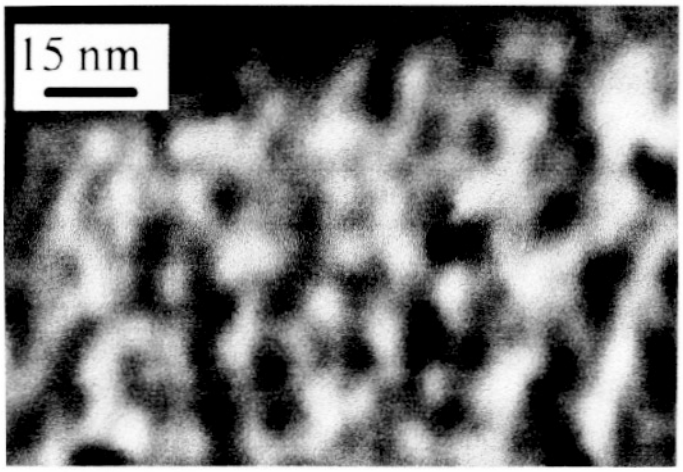

Figure 2. An XTEM micrograph illustrating the microstructure of porous amorphous Si ($c = 4$ at.%, $j = 15$ mA cm^{-2}, $t = 12$ s).

Cross-section transmission electron microscopy (XTEM) was used to examine the structure of the samples. Figure 2 is a XTEM micrograph which illustrates the microstructure of porous Si formed in the amorphous layer ($j = 15$ mA cm^{-2}, $t = 12$ s). One can see that amorphous PS has a wire-like structure with a cross-sectional dimension of the wires of 5–10 nm.

The topography of the surface was observed by scanning tunnelling microscopy (STM). We used our prototype of the WA Technology Mini CryoSTM with cut gold tips. On the medium scale, the surface exhibited 40–80 nm features with a corrugation amplitude of about 10 nm, which were superimposed on much larger structures of a few hundred nanometres in size and with a corrugation height of about 50 nm. On the nanometre scale, which is generally associated with the porous structure of PS [5–9], the surface exhibited protruding features, which were distributed uniformly with average size varying over different areas between 3 and 9 nm and with a corrugation amplitude of 1–3 nm. The real size of the quantum wires near the surface is likely to be somewhat smaller than the imaged features, which are subject to broadening due to the finite size of the STM tip. The hillock distribution did not exhibit any preferential orientation or symmetry, as confirmed by FFT analysis of the images. A typical image (a sample with $c = 4$ at.%, $j = 15$ mA cm^{-2}, $t = 6$ s) is shown in figure 3 with the corresponding line profile between points A and B. Apparently, the STM results are in excellent agreement with the XTEM observations. The results also correspond well to other authors' observations of heavily doped crystalline PS both on the micrometre [5, 6] and nanometre [7–9] scales.

In order to have more information on the structure of the layers we have made channelling measurements using backscattering of α-particles with an incident energy of 1.7 MeV (Rutherford backscattering—RBS). The experiments consist of finding the particular geometry for which the incident beam is aligned through the (111) Si substrate direction to

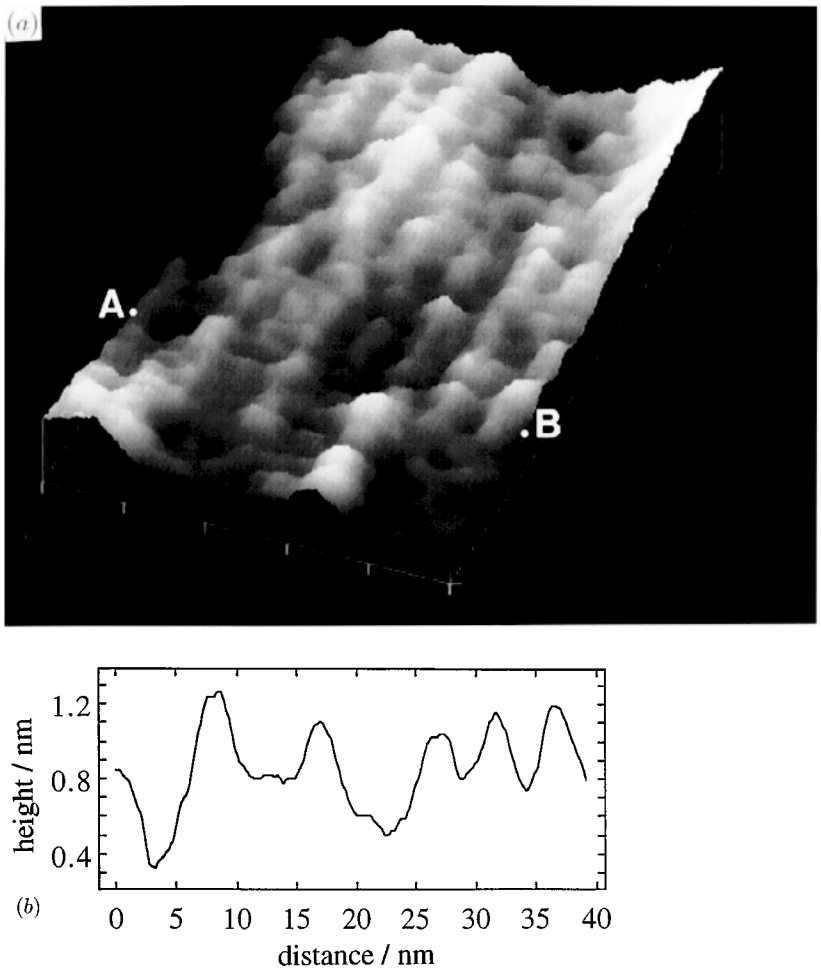

Figure 3. (*a*) An STM constant-current image; 40×40 nm^2 at -600 mV/1 nA ($c = 4$ at.%, $j = 15$ mA cm^{-2}, $t = 6$ s). (*b*) A line profile between points A and B on the image.

analyse the compact (unanodized) and the porous layers. The RBS spectra of the compact 4% sample and of the structure displayed in figure 1(*b*) after etching at $j = 15$ mA cm^{-2} for $t = 24$ s, in random and channelling geometries, are shown in figure 4(*a*). A surface film of SiO_2 with a thickness of about 5 nm is revealed in the a-PS spectra. In contrast to the case of the crystalline counterparts [10], the RBS spectrum in random geometry corresponding to the amorphous porous layer is similar to that for the amorphous compact layer. This is probably due to the absence of significant contamination in the a-PS. The thickness of the a-Si layer determined from the RBS spectrum is found to be $L_0 = 360$ nm. The apparent decrease of a-Si thickness in the aligned spectrum of a-PS corresponds to the presence of the low-density layer (the porous layer). A simulation of RBS data yields a porosity of 59%. Figure 4(*b*) shows the distribution of Mn atoms across the film thickness before and after etching, extracted from RBS spectra. The depth is measured as the atomic number density of scattering centres per unit square ($n \times l \times (1 - P)$, where $n = 5 \times 10^{22}$ cm^{-3} is the atomic number density in the material, and l is the real depth). It is evident that the

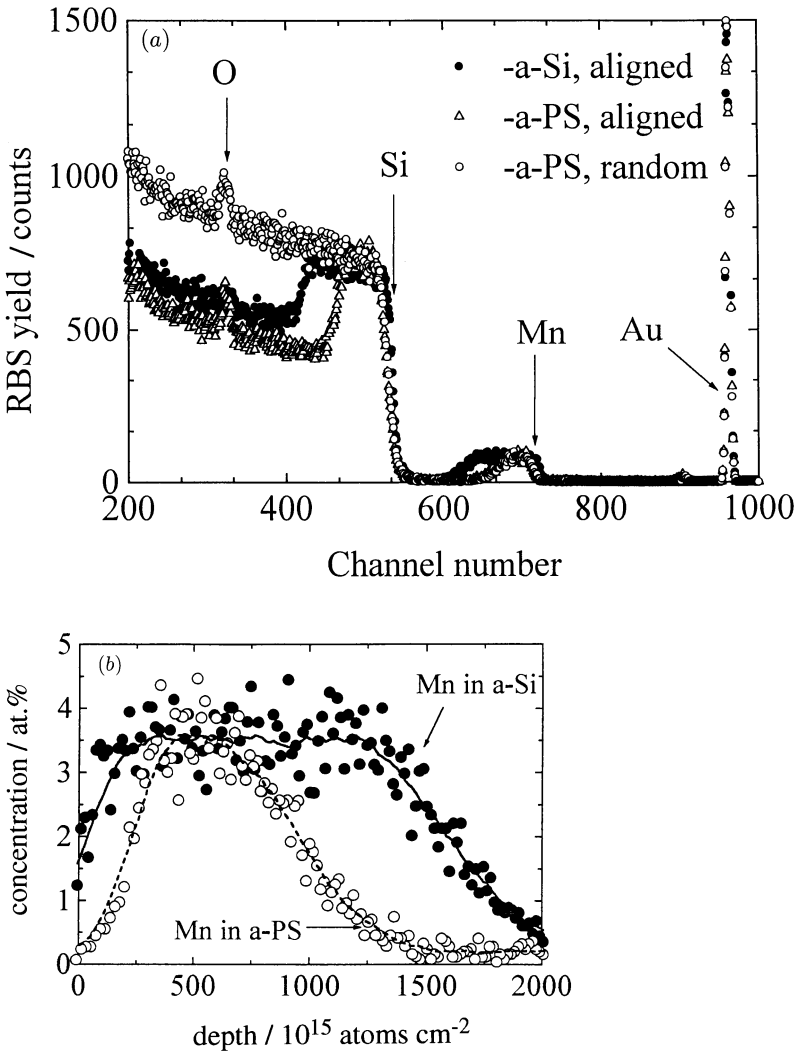

Figure 4. (*a*) Random and aligned RBS spectra of 1.7 MeV ^{4}He ions from the compact and porous a-$Si_{1-0.04}Mn_{0.04}$. (*b*) The depth distribution of Mn atoms in compact and porous a-$Si_{1-0.04}Mn_{0.04}$. The depth is measured by RBS in units of the layer's density of scattering atoms (see the text). Solid lines represent adjacent averaging of experimental points.

maximum Mn concentrations in the compact and porous layers are equal. This implies that there is no redistribution of the impurity after chemical dissolution, in contrast with the case of porous crystalline silicon [11]. It is also important that the peak corresponding to the Au contact on the compact layer coincides with that on the porous layer (figure 4(*a*)). Hence, we may conclude that gold atoms do not penetrate into the pores.

The conductance measurements were made in vertical geometry using a two-terminal dc technique with a Keithley 602 electrometer. The excitation voltage of 3 mV was small enough to ensure ohmic behaviour of current–voltage characteristics. For all structures, at least two different Au dot contacts on the same sample were investigated. No difference in their behaviour (within 3%) over the full temperature range was observed. It was found that,

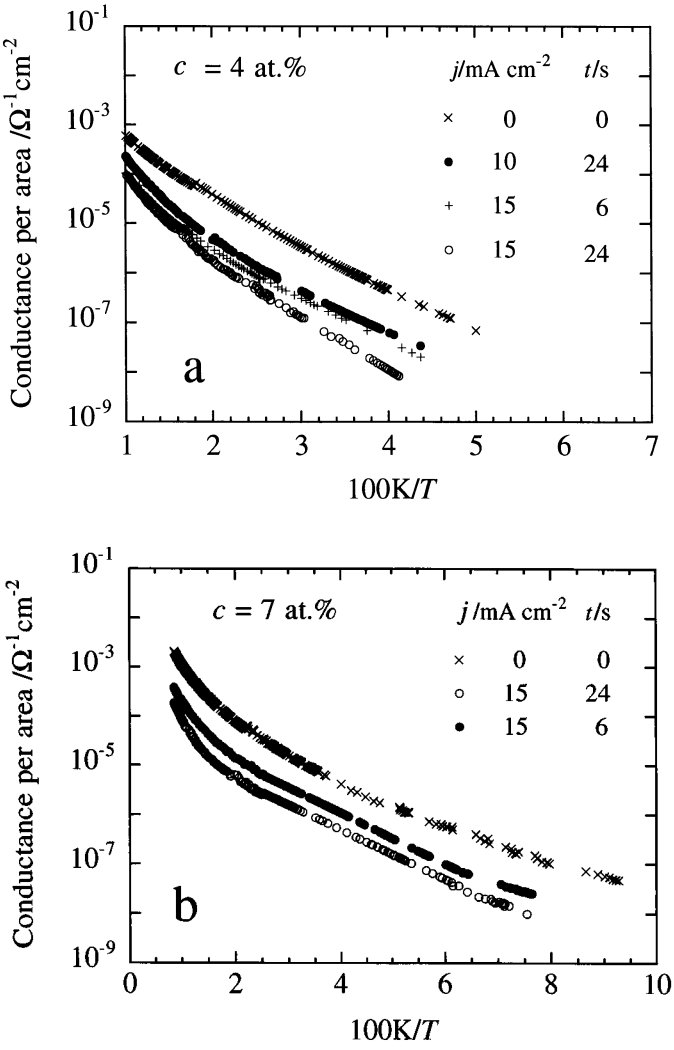

Figure 5. The temperature dependence of the vertical conductance per contact area in samples obtained under different anodization conditions. (a) $c = 4$ at.%, (b) $c = 7$ at.%.

at room temperature, the resistance of the structures does not depend on the thicknesses of the porous layer L (i.e. on anodization time and current) but always has approximately the same value $\sim$200 Ω. This results from the presence of the surface SiO_2 film, whose resistance is in series with the resistance of the PS. However, measurements of the conductance at low temperatures ($T < 100$ K) showed that the impedance increases proportionally L (figure 5). This means that at low temperatures the resistance is due to bulk processes in the PS rather than to junction or interface properties. It is important to note that porous samples have a much larger resistance than do the unanodized films. This means that we can ignore the contribution from the non-etched a-$Si_{1-c}Mn_c$ layer located between the porous layer and the substrate (see figure 1(*b*)). In what follows, we will discuss only the low-temperature data.

3. Experimental results and discussion

It is possible to determine the dimensionality of the system d from measurements of the temperature dependence of the VRH conductivity $\sigma(T)$. The behaviour of the conductivity in the regime of Anderson localization is of the form $\exp[-(T_0/T)^x]$ where the exponent x is given by [12, 13]

$$x = (p+1)/(p+d+1) \qquad \text{in two or three dimensions} \tag{1}$$

and

$$x = 1 \qquad \text{for an infinite 1d chain.} \tag{2}$$

Here p is the power by which the density of states rises from zero at the Fermi level: $g(\epsilon) \propto |\epsilon|^p$. Thus, the value of the hopping exponent x is directly connected with the system's dimension.

In order to find out the values of x at different temperatures, the conductivity data can be analysed by procedure introduced by Zabrodskii and Shlimak [14] and Hill [15], where the local activation energy W is plotted against $1/(kT)$ on a log–log scale:

$$W = -\mathrm{d}(\ln\sigma)/\mathrm{d}(1/kT) = x(kT_0)^x(kT)^{1-x}. \tag{3}$$

This assumes that the temperature dependence of the pre-exponential term is negligible, which usually appears to be the case for $T < 300$ K in amorphous silicon [16], so the gradient of the log–log plot yields the quantity $x - 1$.

Table 1. Regimes of etching, fitting and calculated parameters for variable-range hopping conduction in porous amorphous Si$_{1-c}$Mn$_c$. The table shows the parameters obtained by least-squares fitting to the equation $\sigma = \sigma_0 \exp[-(T_0/T)^x]$ in different intervals of temperature, ΔT_h and ΔT_l. c is the concentration of Mn, j the anodization current density, t the anodization time, g_3 is the 3d density of localized states, calculated from $T_0 = 2.6^4/kg_3a^3$, a is the localization length ($a = 0.4$ nm for $c = 4$ at.% and $a = 0.6$ nm for $c = 7$ at%) and g_1 is the 1d density of localized states, calculated from $\Delta E = 1/2g_1a$.

c/at.%	j/mA cm^{-2}	t/s	ΔT_h/K	x	T_0/K	g_3/eV^{-1} cm^{-3}	ΔT_l/K	x	ΔE/meV	g_1/eV^{-1}cm^{-1}
4	0	0	100–58	0.23	5.1×10^6	1.8×10^{21}	58–13	0.54	$2.4(T/\mathrm{K})^{0.46}$	—
4	15	6	100–30	0.24	1.5×10^7	7.7×10^{20}	30–20	1.02	16	7×10^8
4	15	24	100–38	0.25	2.3×10^7	5.1×10^{20}	38–23	0.92	21	6×10^8
4	10	24	100–23	0.24	1.6×10^7	7.6×10^{20}	—	—	—	—
7	0	0	60–11	0.24	3.3×10^6	2.1×10^{21}	—	—	—	—
7	15	6	65–30	0.24	4.6×10^7	1.3×10^{21}	30–18	1.01	11	8×10^8
7	15	24	100–53	—	—	—	33–18	0.95	10	9×10^8

The temperature dependence of the conductance per unit area ($\sigma = I/VS$, where $S = 5 \times 10^{-3}$ cm^2 is the contact area) at $T < 100$ K for compact a-Si samples and for samples after the formation of porous layers is shown in figure 5. Figure 6 shows results obtained by a procedure of graphical differentiation of the $\sigma(T)$ data for unanodized samples and for PS obtained under different anodization conditions. A list of results of least-squares fits of equation (3) to the $\sigma(T)$ data are presented in table 1. For compact samples ($j = 0$) it is found that $x \approx 1/4$ for $T = 100$–58 K and $x \approx 1/2$ for $T = 58$–13 K for the 4% sample, and $x \approx 1/4$ for $T = 60$–11 K for the 7% sample. The $T^{-1/2}$-law found for the 4% sample at low temperatures is usually attributed to the presence of a parabolic Coulomb gap ($p = 2$) in the density of localized states (DLS) near the Fermi level as originally proposed by Efros and Shklovskii [17]. The absence of this dependence above 11 K for the 7%

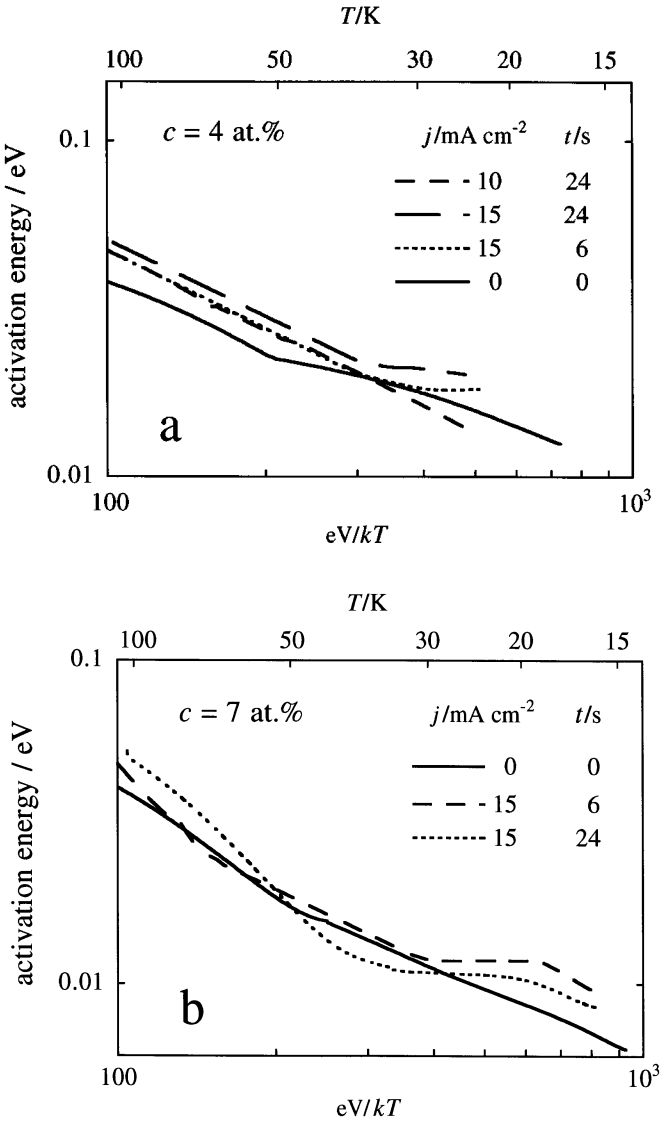

Figure 6. The activation energy W plotted against $(kT)^{-1}$ on double-logarithmic scales for the PS obtained under different anodization conditions. The slopes correspond to $x-1$, where x is the hopping exponent; (a) $c = 4$ at.%, (b) $c = 7$ at.%.

sample is probably related to increased screening of the electron–electron interaction nearer the metal–insulator transition which restricts Coulomb gap behaviour to lower temperatures.

As temperature is reduced below 30–38 K, there appears to be a crossover from an $\exp[-(T_0/T)^{1/4}]$ Mott form to a simply activated law, $\exp(-\Delta E/kT)$, in the samples treated with 15 mA cm^{-2} anodic current density. The T^{-x}-dependence with x changing from 1/2 to 1 with decreasing temperature below 6 K has been observed in a-$Si_{1-c}Mn_c$ compact films ($c \geqslant 9$ at.%) in a 3d VRH regime after annealing [18]. The films were evaporated on glass substrates and conductivity was measured in the plane of the samples.

This behaviour was explained by the presence of a 'hard' magnetic gap in the density of localized states caused by the s–d exchange interaction between the hopping electrons and localized spins on Mn clusters. Since, in the present case, the unanodized samples do not exhibit such a crossover we must exclude magnetic correlations from the interpretation of $\sigma(T)$ data for PS. Moreover, this exclusion is supported by the observation of a T^{-1}-law for undoped amorphous PS [4].

The crossover observed in this work is attributed to a temperature-induced transition from 3d to 1d VRH conduction. It is easy to understand this phenomenon for an isolated infinite silicon pillar with diameter D. A specific feature of the VRH process is the increase of the optimum hopping length R_{opt} as temperature is lowered. Hence, anisotropy of the resistance associated with hops along and transverse to the pillar should appear and the effective dimensionality of the system should be reduced when the maximum hopping length on the percolative cluster R_{max} becomes larger than D (figure 1(a)). In the opposite case, conduction must follow the usual Mott behaviour for three dimensions. From the condition $D \sim R_{\mathrm{max}} = (a/2)(T_0/T^*)^{1/4}$, where a is the localization length and T^* is the temperature of the transition, we can estimate the mean diameter of the silicon columns in PS. Using values for the localization length determined, for films of the same concentrations, by analysis of variable-range hopping in the Coulomb gap [19]: $a = 0.4$ nm for $c = 4$ at.% and $a = 0.6$ nm for $c = 7$ at.%, $T^* = 30$–38 K, and taking T_0 from table 1, we find that $D \sim 5$–6 nm. This value is in excellent agreement with our XTEM and STM results presented in figures 2 and 3. The sample formed with the smallest anodic current density ($j = 10$ mA cm^{-2}) does not exhibit a transition to the 1d regime down to 23 K. We assume that in this sample the diameter of the silicon pillars is larger than R_{max}(at $T = 23$ K) $= 5.8$ nm.

Various models have been proposed for VRH conduction in disordered 1d systems. The works of Kurkijarvi [20], Raikh and Ruzin [12] and Hunt [13] relate to single 1d chains. Shante [21] and Zvyagin [22] applied percolation arguments to describe transport through a large number of parallel chains with rare weak interconnections. Obviously, the latter two models are more appropriate here. In spite of the different approaches to the theory of 1d hopping, the final results obtained by the different authors are very similar: for the infinite 1d disordered chain case

$$\sigma(T) \sim \exp(-\Delta E/kT) \tag{4}$$

$$\Delta E = (Cg_1 a)^{-1} \tag{5}$$

where C is a numerical factor and g_1 is the 1d DLS. A value of $C = 2$ was evaluated by an optimization procedure by Raikh and Ruzin [12], and independently by Zvyagin [22]. Zvyagin proposed that his result should be applied directly to PS. He predicted a strong anisotropy of conductivity for the quasi-1d system consisting of a network of parallel wires with weak interconnections at temperatures below $T_{\mathrm{C}} = 2\Delta E/k\sqrt{D/a}$. Using $\Delta E = 10$–20 meV and $D \sim 8$ nm (the mean value in figure 2), we find $T_{\mathrm{C}} = 1000$–2000 K in the different samples. This value is high enough for us to consider porous a-$Si_{1-c}Mn_c$ as a quasi-1d system.

We can check the 1d hopping model by making a quantitative analysis of parameters which can be extracted from $\sigma(T)$ data. From equation (5), we can estimate g_1, the one-dimensional DLS. The 3d density of states g_3 can be calculated from the high-temperature data where Mott's law is valid: $g_3 = B^4/kT_0a^3$, where [23] $B = 2.6$. Results of the calculations are given in table 1. On the other hand, the parameters g_1 and g_3 must obviously be connected by the relation $g_1 \approx g_3 D^2$. Using the experimental values of g_3, a and $D \sim 8$ nm, we have $g_1 = (4{-}9) \times 10^8$ eV^{-1} cm^{-1} which is similar to the values

obtained from the low-temperature conductivity data, $g_1 = (6-9) \times 10^8$ eV^{-1} cm^{-1}.

One can see that the two conduction regimes (3d and 1d) shade into one another without any gradient discontinuity (figure 6 is smooth at T^*). Matching the typical hopping lengths R extracted from 3d and 1d behaviour gives another way of checking the model. The value of R in the 3d VRH model is given by $R_{3d} = 0.25a(T_0/T)^{1/4}$. The resistivity of a disordered 1d chain is determined by exponentially rare breaks, regions within which the local density of localized states is anomalously small [20]. According to Raikh and Ruzin [12], the hopping distance in the break is given by $R_{1d} = (2g_1kT)^{-1}$. Using the experimental values of T_0, T^*, a and g_1 taken from table 1 for the sample with $c = 4$ at.%, $j = 15$ mA cm^{-2}, $t = 6$ s, we obtain a good agreement: $R_{3d}(T^*) = 2.7$ nm and $R_{1d}(T^*) = 2.6$ nm.

One can see from figure 6(b) that for 7% PS samples at low temperatures ($T < 18$ K) the activation energy depends on temperature again. There are two possible explanations for this. Firstly, we may be seeing a reversion to 3d behaviour as electrons start to hop between wires. The wires are not totally isolated from one another so, when hopping distances along the wires become sufficiently large with correspondingly small transition probabilities, transverse tunnelling can become significant. The hopping then becomes 3d (though anisotropic) and the conductivity returns towards the Mott $x = 0.25$ form. This will occur when [22]

$$T \ll \frac{2\Delta E}{k}\left(\frac{a}{D_1}\right)^2. \tag{6}$$

For $a = 0.6$ nm, $D_1 \approx D$ (for porosity of about 50%) and $\Delta E = 10$ meV, we have the result $T \ll 2.3$ K. This temperature is too low.

The second possibility is that, as the hopping distance increases, the columns no longer behave as *infinite* 1d wires but as mesoscopic systems in which the conductivity becomes determined by optimum trajectories. This results in a complicated temperature-dependent activation energy. Following the calculation of Raikh and Ruzin [12], the dependence of W on T should appear when

$$\frac{2L}{a}\exp\left(-\frac{\Delta E}{kT}\right) \ll 1. \tag{7}$$

For $L = 0.2$ μm, we obtain the quite acceptable result $T \ll 19$ K.

It is of interest that the 3d density of states in porous samples is smaller than that in compact samples. The larger the anodic current or anodization time, the smaller the 3d DLS becomes. Since the manganese concentrations in a-Si and in porous a-Si layers are equal, we attribute this effect to broadening of the impurity band by quantum confinement in the silicon wires. Bastard [24] was the first to calculate the binding energy of a localized level in a quantum well as a function of well size and of the impurity position in the well. It was found that the ground-state degeneracy of the impurity site is lifted. In contrast with the case for homogeneous materials, the confinement effect leads to a spreading of impurity levels which depends upon the impurity position. As a result, the width of the impurity band in PS will increase and the density of states will decrease as the diameter of the silicon columns is reduced. Also, this effect will be intensified by the statistical spread of pore sizes which is usually found in similar regimes of etching [25].

There is one problem which deserves further investigation. The question is why the Coulomb correlations observed in the compact 4% sample are not seen in the corresponding porous material. We suggest that the reduced average volume density of localized states in the porous material may reduce the width of the Coulomb gap [17] and hence it is not observed in the temperature range of our experiments.

4. Conclusion

The conductivity of porous a-$Si_{1-c}Mn_c$ samples ($c = 4$ and 7 at.%) shows a crossover from the $\exp[-(T_0/T)^{1/4}]$ Mott form to a simply activated law, $\exp(-\Delta E/kT)$, as temperature is reduced below 30–38 K. This behaviour is attributed to a temperature-induced transition from 3d to 1d hopping conduction in the silicon wires of the porous material. We have observed a decrease of the density of states in PS which we have explained in terms of a broadening of the impurity band caused by the lateral confinement.

Acknowledgments

AY is grateful to the NATO Expert Visit Grant (HTECH.EV 951113) for financial support that enabled him to carry out research in Cambridge. AD is grateful to the Research Centre Rossendorf for having provided him with financial support during his stay in Dresden for RBS studies. CJA and VZC acknowledge the technical support of WA Technology and financial support of VZC through the Committee of Vice-Chancellors and Principals Overseas Research Student Scheme, and by the Cambridge Overseas Trust and the Taylor Fund. This work was also supported in part by the International Science Foundation through the Grants Nos U-88 000 and U-88 300, and by INTAS (Grant No 94-4435). We thank Dr A K Gutakovskii for the electron microscopy results presented in this paper.

References

[1] Canham L T 1990 *Appl. Phys. Lett.* **57** 1046
[2] Lehmann V and Gosele U 1991 *Appl. Phys. Lett.* **58** 856
[3] Webb R A, Fowler A B, Harstein A and Wainer J J 1986 *Surf. Sci.* **14** 170
[4] Yakimov A I, Stepina N S, Dvurechenskii A V and Scherbakova L A 1995 *Physica* B **205** 298
[5] Amisola G B, Behrensmeier R, Galligan J M, Otter F A, Namavar F and Kalkoran N M 1992 *Appl. Phys. Lett.* **61** 2595
[6] Enachescu M, Hartmann E and Koch F 1994 *Appl. Phys. Lett.* **64** 1365
[7] Dumas P, Gu M, Syrykh C, Gimzewski J K, Makarenko I, Halimaoui A and Salvan F 1993 *Europhys. Lett.* **23** 197
[8] Ito K, Ohyama S, Uehara Y and Ushioda S 1995 *Appl. Phys. Lett.* **67** 2536
[9] Gomez-Rodriguez J M, Baro A M and Parkhutik V P 1990 *Appl. Surf. Sci.* **44** 185
[10] Grosman A, Ortega C, Siejka J and Chamarro M 1993 *J. Appl. Phys.* **74** 1992
[11] Karanovich A A, Romanov S I, Kirienko V V, Myasnikov A M and Obodnikov V I 1995 *J. Phys. D: Appl. Phys.* **28** 2345
[12] Raikh M E and Ruzin I M 1989 *Zh. Eksp. Teor. Fiz.* **95** 1113 (Engl. Transl. 1989 *Sov. Phys.–JETP* **69** 642)
[13] Hunt A 1993 *Solid State Commun.* **86** 765
[14] Zabrodskii A G and Shlimak I S 1975 *Fiz. Tekh. Poluprov.* **9** 587 (Engl. Transl. 1975 *Sov. Phys.–Semicond.* **9** 391)
[15] Hill M 1976 *Phys. Status Solidi* a **35** K29
[16] Pfeisticker R, Kalbitzer S and Muller G 1981 *Nucl. Instrum. Methods* **1182+1183** 603
[17] Efros A L and Shklovskii B I 1975 *J. Phys. C: Solid State Phys.* **8** L49
[18] Yakimov A I, Wright T, Adkins C J and Dvurechenskii A V 1995 *Phys. Rev.* B **51** 16 549
[19] Dvurechenskii A V and Yakimov A I 1995 *Jubilee Collection of the Institute of Semiconductor Physics* ed I G Neizvestny (Novosibirsk: Nauka)
[20] Kurkijarvi J 1973 *Phys. Rev.* B **8** 922
[21] Shante V K S 1977 *Phys. Rev.* B **16** 2597
[22] Zvyagin I P 1995 *Zh. Eksp. Teor. Fiz.* **107** 175 (Engl. Transl. 1995 *Sov. Phys.–JETP* **80** 93)
[23] Seager C H and Pike G E 1974 *Phys. Rev.* B **10** 1435
[24] Bastard G 1981 *Phys. Rev.* B **24** 4714
[25] Herino R, Bomchil G, Barla K, Bertrand C and Ginoux J L 1987 *J. Electrochem. Soc.* **134** 1994